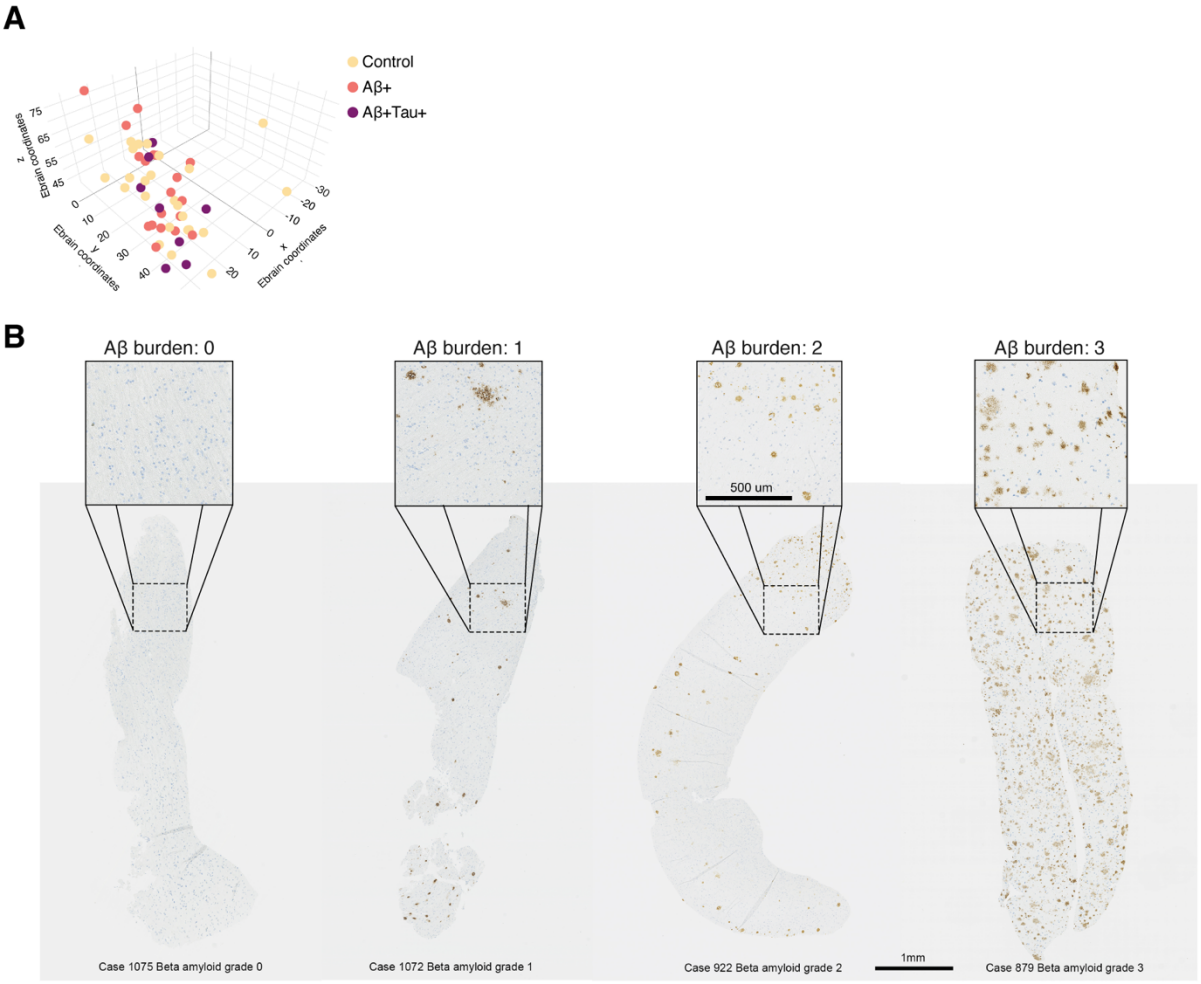

Figure S1. Stereological positioning and neuropathological scoring of biopsy cohort samples
A) *Relative three-dimensional coordinates of biopsy positions based on the mapping of post-surgical CT or MRI images from 52 subjects. Samples are colored by AD pathologic status.* ***B)*** *Representative images of biopsies with different Aβ burden.*

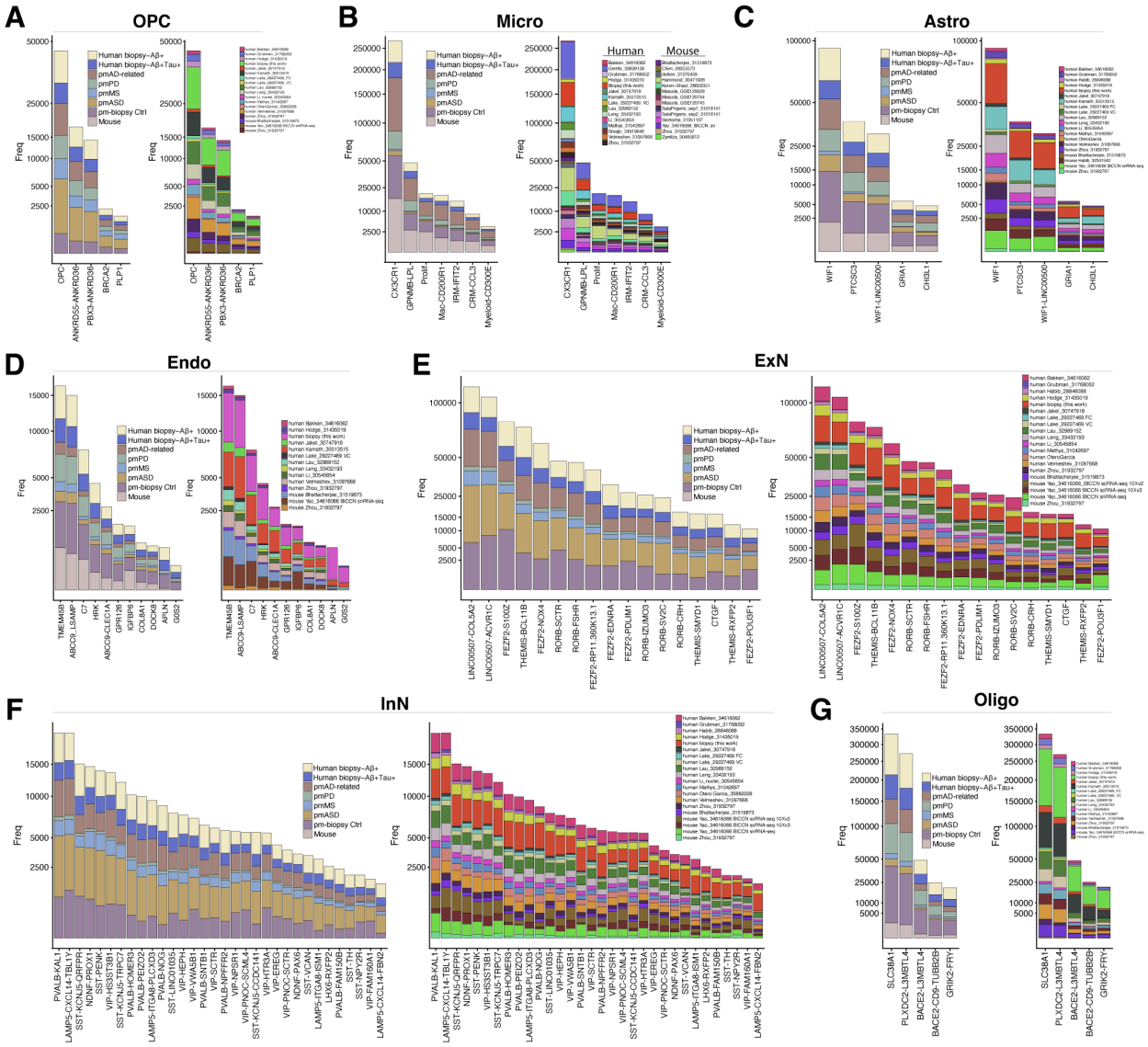

Figure S2. Individual cell types in the integrative analysis are well represented across biological conditions and datasets

A-G) *Number of cells in each cell type stratified by biological condition (left), and dataset (right). pm, postmortem; PD, Parkinson's disease; MS, multiple sclerosis; ASD, autism spectrum disorder.*

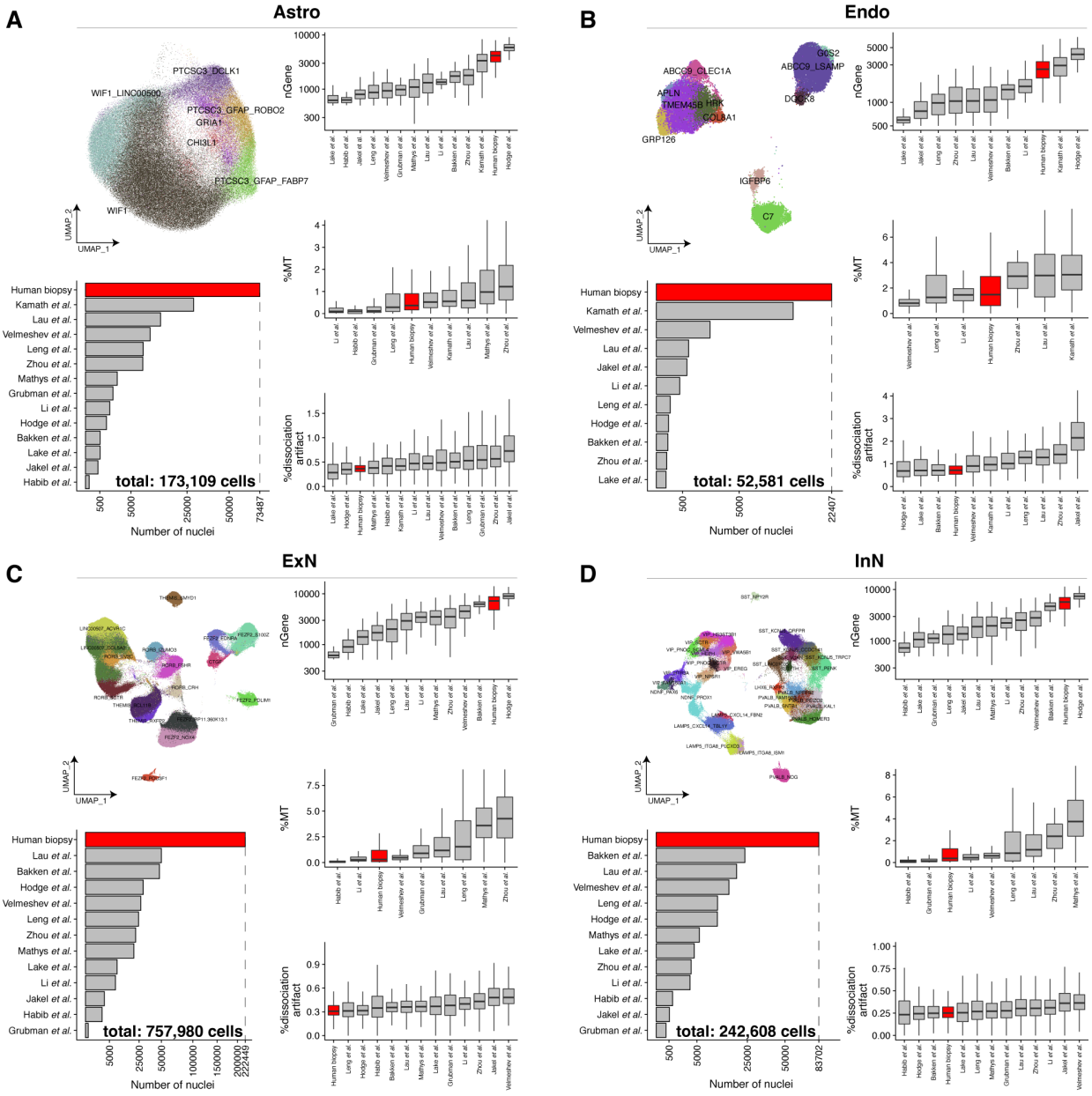

Figure S3. Quality metrics of human datasets included in the integrative analysis of Astro, Endo, ExN, and InN cell classes

A-D) *QC metrics of human datasets parsed by major cell class:* ***A)*** *Astrocytes,* ***B)*** *Endothelial cells,* ***C)*** *Excitatory neurons,* ***D)*** *Inhibitory neurons. Detailed marker analysis results are provided in* ***Table S3****. More QC metrics are available through the linked portal (see data availability section). %MT: percent expression of genes per cell that map to mitochondrial genes, normalized by nUMI. %dissociation artifact: percent expression of dissociation-related artifactual genes[20] in each nuclei and normalized by nUMI. Astrocyte PTCSC3 cell type is more deeply clustered into three states (PTCSC3-DCLK1,PTCSC3-GFAP-ROBO2, and PTCSC3-GFAP-FABP7). Center line, median; box limits, upper and lower quartiles; whiskers, 1.5x interquartile range.*

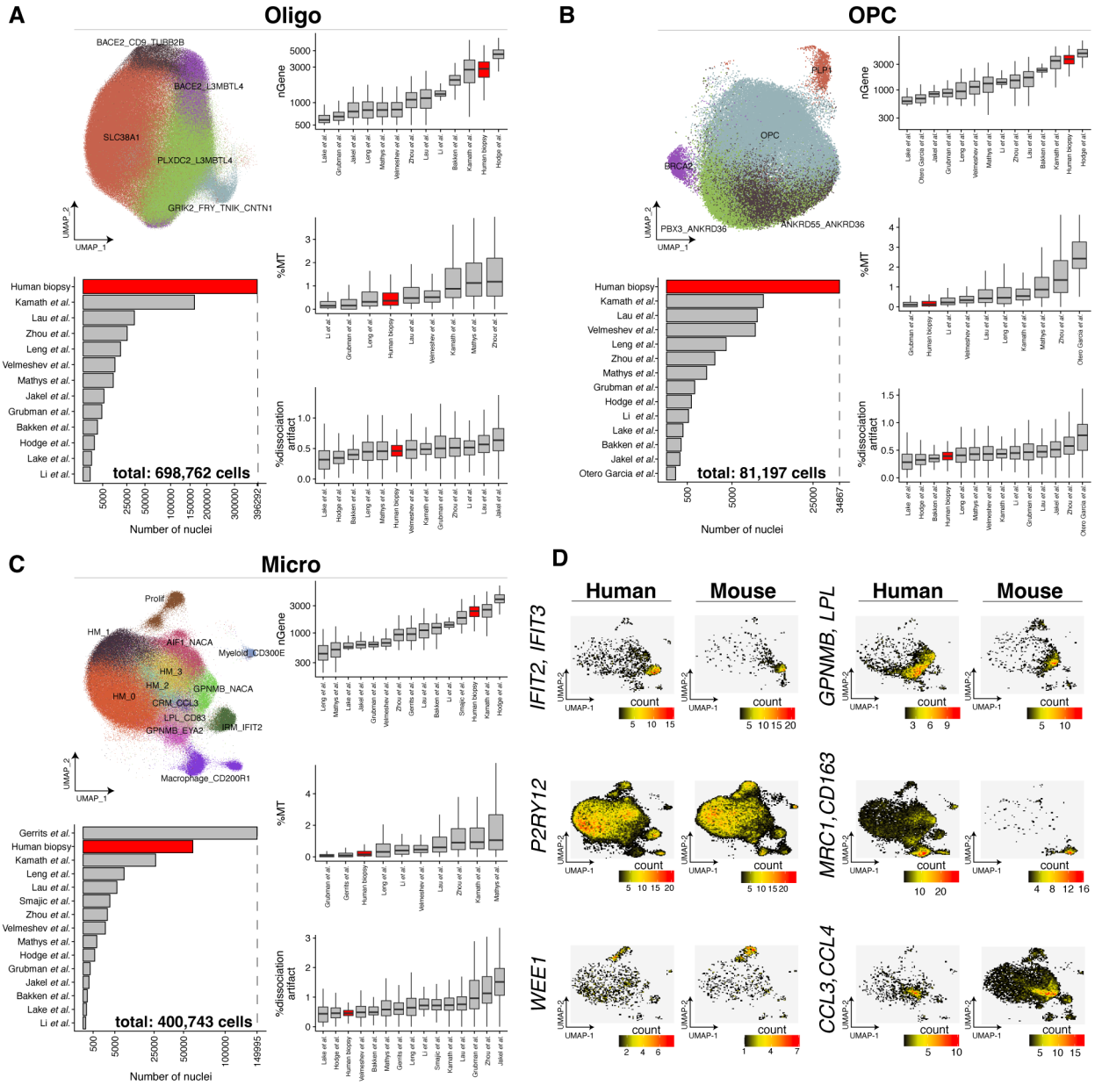

Figure S4. Quality metrics of human datasets included in the integrative analysis of Oligo, OPC, and Micro cell classes

QC metrics of human datasets parsed by the major cell class: ***A)*** *Oligodendrocytes,* ***B)*** *Oligodendrocyte progenitor cells, and* ***C)*** *Microglia.* ***D)*** *Comparisons of some key microglia states between human and mouse datasets. Color indicates the number of human or mouse donors that support the expression of the gene in a given UMAP coordinate across datasets. Detailed marker analysis results are provided in* ***Table S3****. More QC metrics are available through the linked portal (see data availability section). %MT: percent expression of mitochondrial genes in each cell and normalized by total nUMI. %dissociation artifact: percent expression of dissociation-related artifactual genes in each cell and normalized by total nUMI. Microglia cell types CX3CR1 and GPNMB-LPL are more deeply clustered into five (HM-0 to HM-4) and three (LPL-CD83 ,GPNMB-EYA2, GPNMB-NACA) states, respectively. Center line, median; box limits, upper and lower quartiles; whiskers, 1.5x interquartile range.*

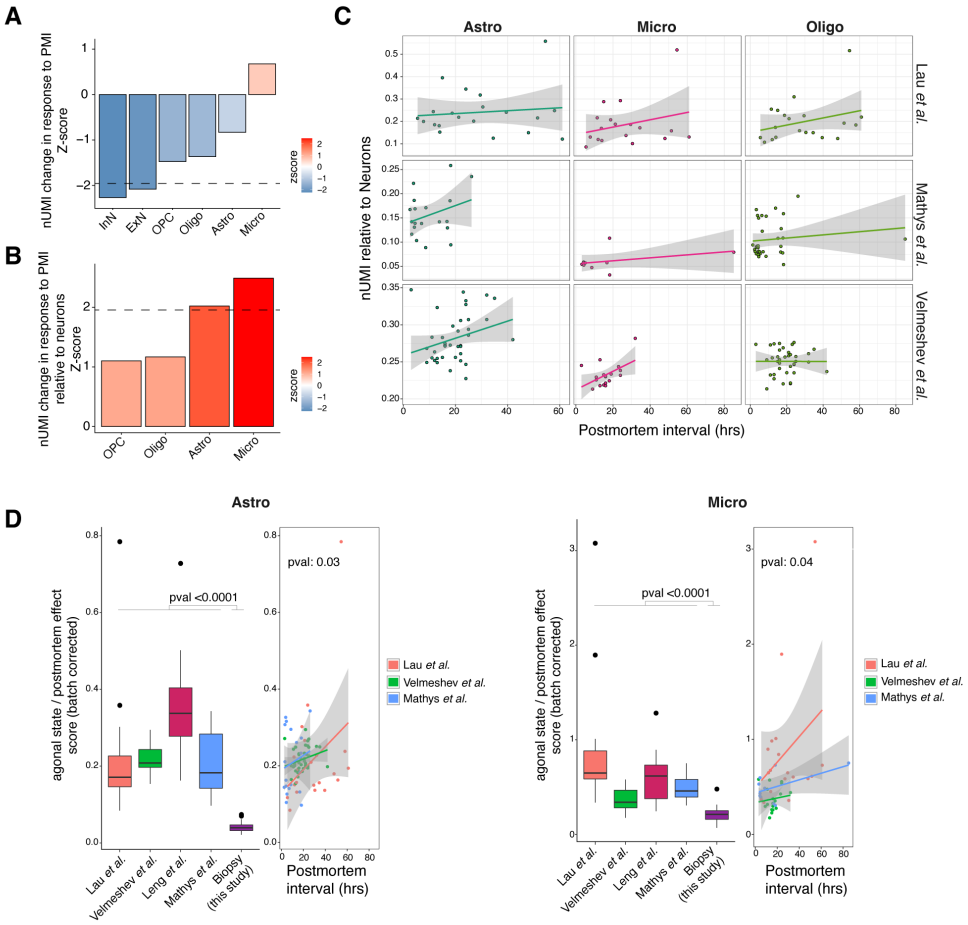

Figure S5. Peri- and post-mortem effects on gene expression patterns

A) *Impact of postmortem interval on the number of expressed transcripts (nUMI) per cell class. To estimate significance within each postmortem dataset, a regression line was fit to estimate the significance of association between PMI and the mean nUMI in each subject. For this analysis, we considered three postmortem datasets of Lau et al., Mathys et al., and Velmeshev et al. that their postmortem interval information were available and had sufficient range for a regression analysis. The p-values from each dataset were next combined using Stouffer's method. To calculate the nUMIs per cell, we excluded the top 50 expressed genes in each dataset to better capture the impact of the postmortem intervals on the expression of the lower expressed genes. The dashed line represents the p-value cutoff threshold of 0.05.* ***B)*** *Impact of PMI on glial-to-neuronal gene expression ratio. Within each of three postmortem datasets, Similar to panel A, a regression line was fit to examine the impact of the PMI on the mean ratio of glial-to-neuronal genes in each subject. The p-values were next combined using Stouffer's method. In each subject, the mean neuronal expression was calculated as the mean nUMI of excitatory and inhibitory neurons, excluding the top50 expressed genes. The dashed line represents the p-value cutoff threshold of 0.05.* ***C)*** *Glial-to-neuronal gene expression ratio as a function of PMI in each of the three postmortem datasets.* ***D)*** *Comparison of glial-to-neuronal gene expression levels between the biopsy and four postmortem datasets. Glial expression in each dataset was normalized to reduce the effect of the ambient RNA as measured by the expression level of the top 250 most specific markers of excitatory and inhibitory neurons. The neuronal specific gene markers were identified based on the pct.1 - pct.2 difference in our biopsy dataset. As shown, this normalization resulted in overlay of agonal state /postmortem scores for samples with a similar PMI across datasets.*

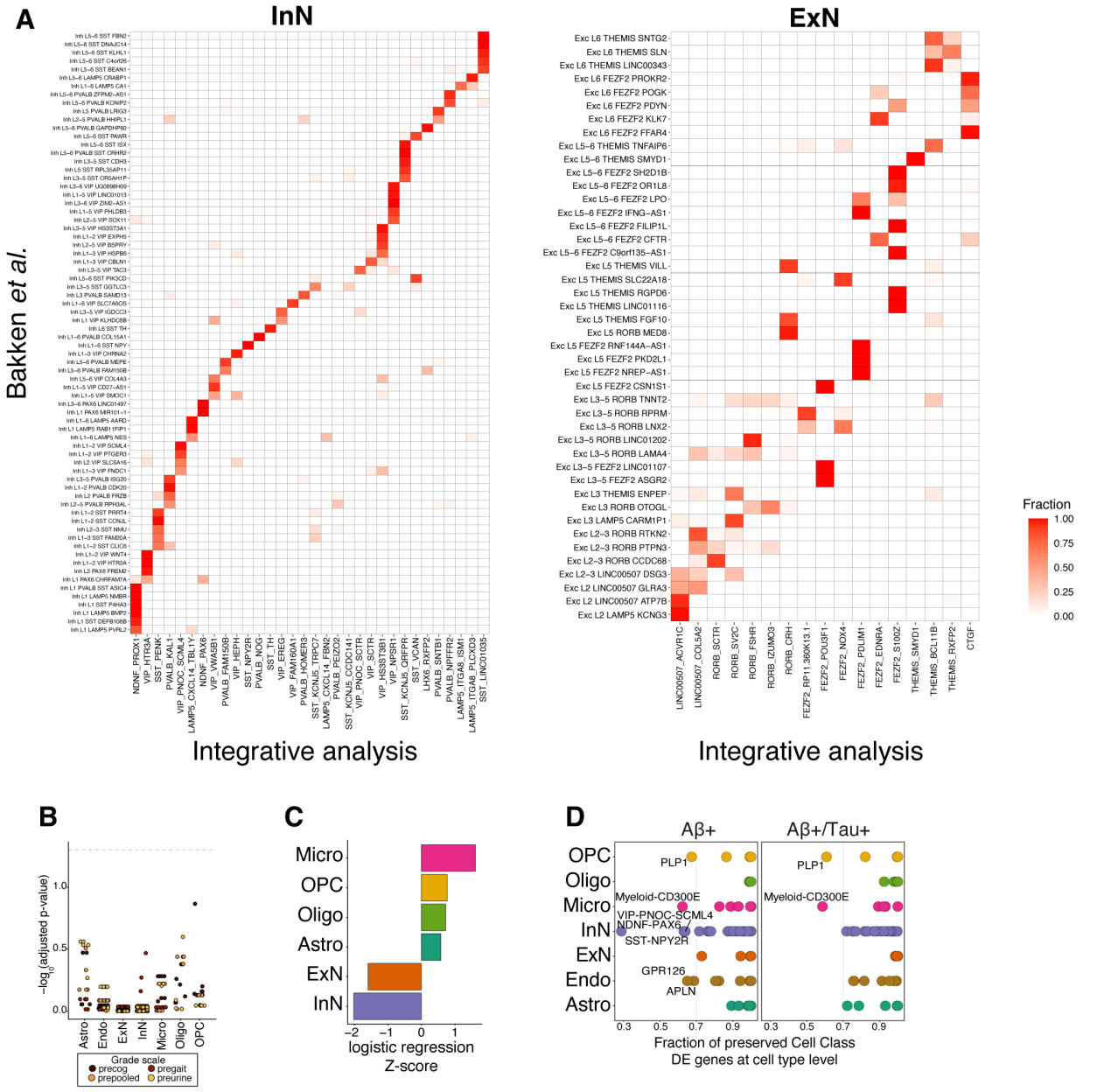

Figure S6. Correspondence of neuronal cell types from integrative analysis with a reference dataset containing cortical layer annotations

A) *The plots represent the correspondence of neuronal cell type annotations from our integrative analysis with cell cluster annotations from a human cortex dataset*[21] *that included cortical layer information. The sum of fractions in each row adds up to one.* ***B)*** *Dot plot of -log*$_{10}$*-transformed FDR-adjusted p-values from logistic mixed-effect model testing association of cell type abundance with iNPH GS (**Methods**) subscore severity measured prior to shunt placement (precog = cognitive subscale, pregait = gait subscale, preurine = urine subscale, prepooled = combined iNPH GS score).* ***C)*** *Z-score from meta-analysis of cell class level differential abundance comparing late-stage samples (Braak V-VI and Aβ+Tau+) versus pathology-free samples (Methods).* ***D)*** *Cell class level DE genes are preserved within cell types. Cell types are labeled in which less than 70% of cell class level DE genes were preserved.*

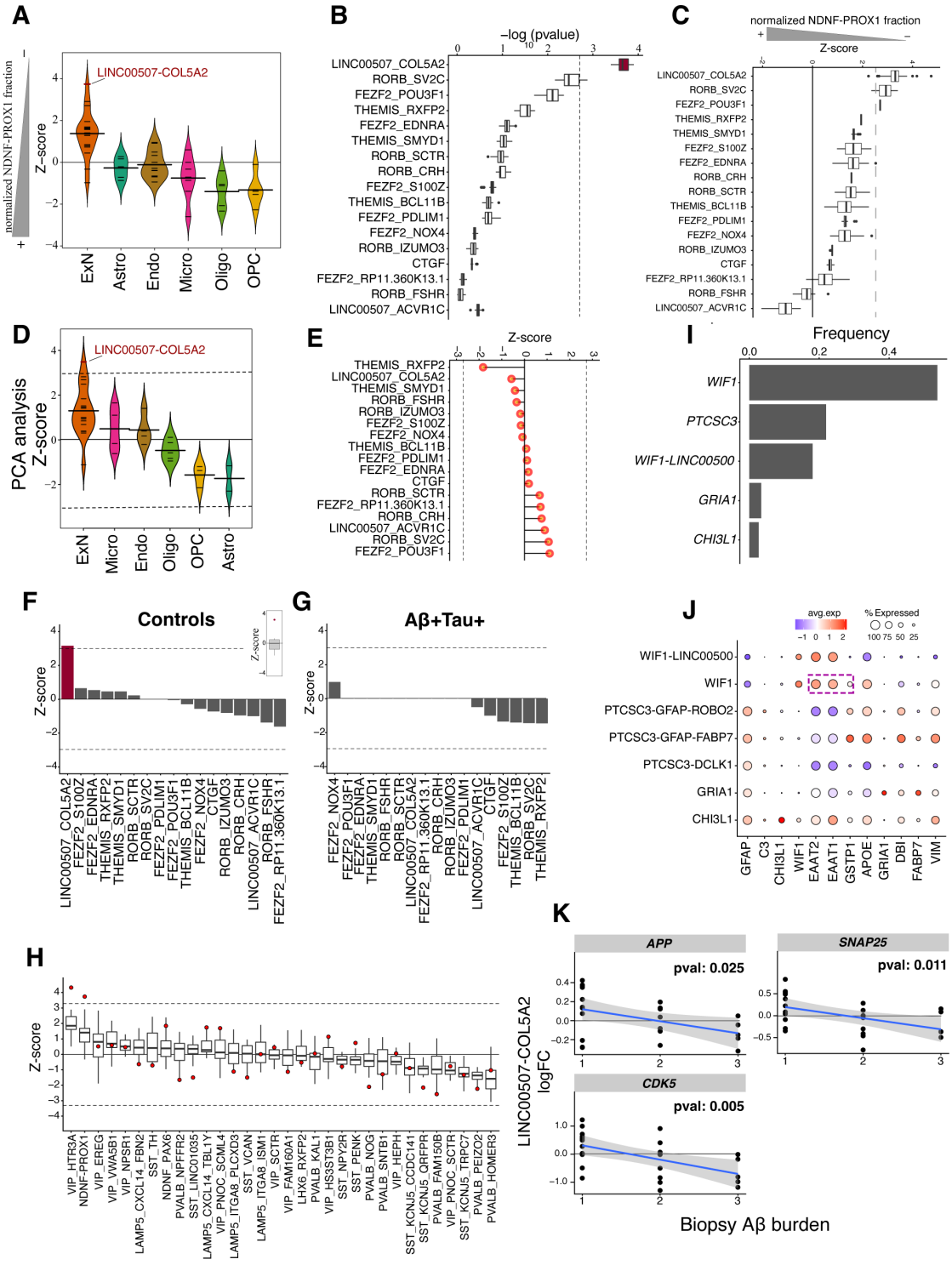

Figure S7. Loss of NDNF-PROX1 inhibitory neurons is associated with an upregulation of excitatory neuron DE signature

A) *Distribution of Z-scores per cell class for the analysis shown in* ***Figure 3A****. Each small line indicates one cell type and the tick lines represent the mean.* ***B)*** *Logistic mixed-effect model regression (Methods) of NDNF-PROX1 proportion versus ExN cell type transcriptional signature in Aβ+ subjects with added*

poisson noise. Poisson noise counts were added to the UMI counts of each gene in each cell prior to computing the regression. Boxplots show the distribution of -log$_{10}$ transformed p-values over 30 noise iterations. Center line, median; box limits, upper and lower quartiles; whiskers, 1.5x interquartile range; points, outliers. ***C)*** *Logistic mixed-effect model regression of NDNF-PROX1 proportion versus ExN cell type transcriptional signature in Aβ+ subjects with downsampling of cells. Iterating 30 times, we randomly downsampled each ExN type to 7000 cells, unless the cell type size was less than this number. Boxplots show the Z-score distributions over the 30 downsampling iterations. The dashed line indicates the FDR threshold of 0.05. Center line, median; box limits, upper and lower quartiles; whiskers, 1.5x interquartile range; points, outliers.* ***D)*** *Association between NDNF-PROX1 loss and LINC00507-COL5A2 cell type assessed using an alternative strategy of constructing a meta gene of the ExN DE signature from the first principal component (Methods). Each small line indicates one cell type and the tick lines represent the mean.* ***E)*** *Logistic mixed-effect model regression of NDNF-PROX1 proportion versus ExN cell type transcriptional signature in Aβ+ subjects after randomizing assignment of cells to excitatory cell types. Dashed line represents FDR-threshold of 0.05.* ***F-G)*** *Logistic mixed-effect model regression (Methods) of NDNF-PROX1 proportion versus ExN cell type transcriptional signature in control (**F**) and Aβ+Tau+ (**G**) subjects. The inset boxplot in **F** shows the overall distribution of Z-scores among the 17 excitatory neuron types. Dashed line represents FDR-threshold of 0.05.* ***H)*** *Boxplots representing the association (as measured by Z-score from logistic mixed-effect model regression) between each inhibitory neuron cell type (x-axis) with the ExN DE signature across 17 ExN types (boxplots). The red dot represents the Z-score of the LINC00507-COL5A2 type. Analysis is based on Aβ+ individuals only. In boxplots, center line, median; box limits, upper and lower quartiles; whiskers, 1.5x interquartile range.* ***I)*** *Barplots representing the relative frequencies of the five astrocyte cell types.* ***J)*** *Dot plots showing expression of astrocyte marker genes in each astrocytic cell type.* ***K)*** *logFC expression of APP, CDK5, and SNAP25 genes in LINC00507-COL5A2 excitatory neurons across increasing Aβ burden scores. Regression line is illustrated in blue with associated standard error.*

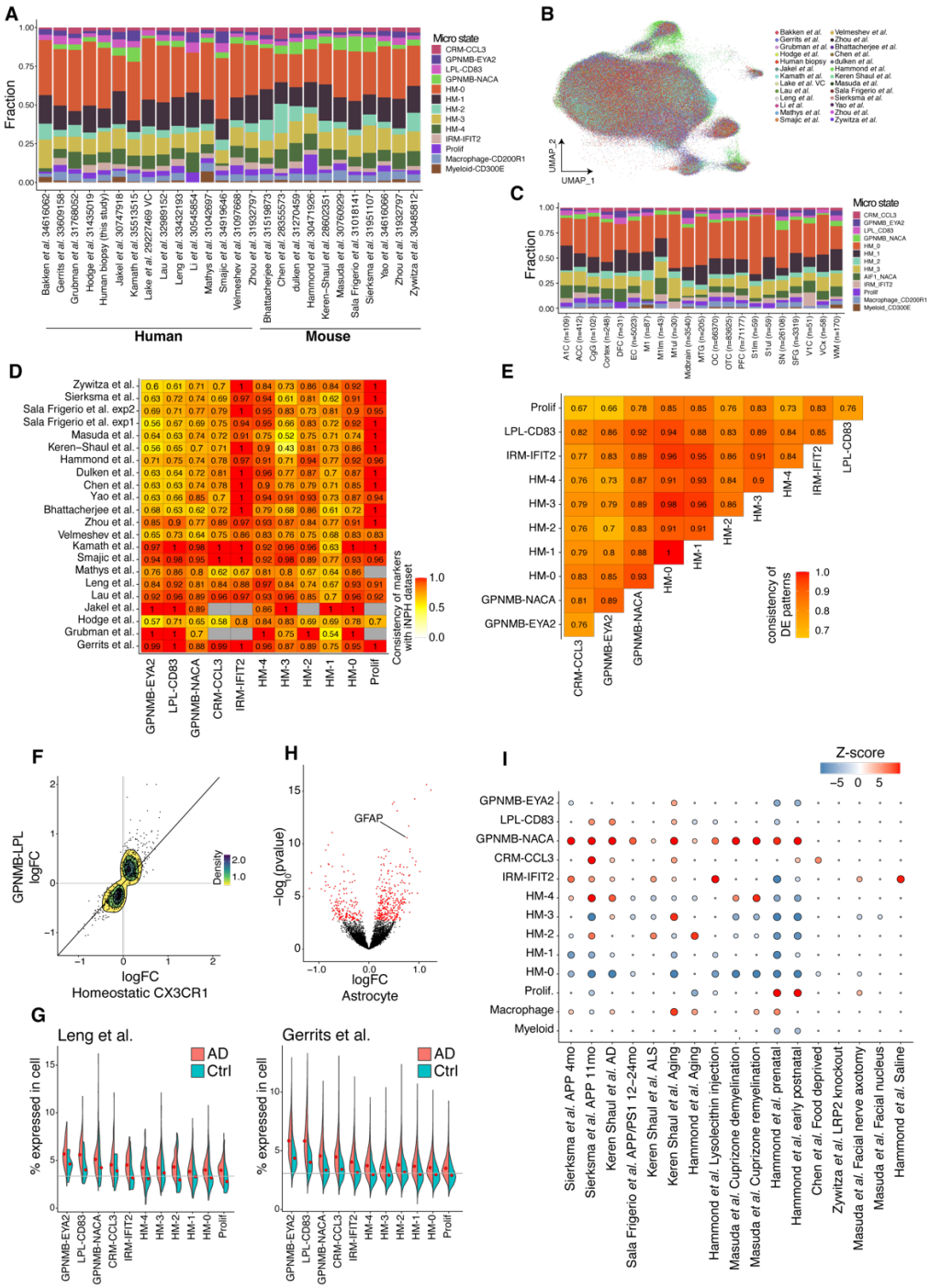

Figure S8. Microglia responses to the accumulation of Aβ and tau in cortical tissue.
A) *Microglia cell state compositions across human and mouse datasets.* ***B)*** *UMAP representation of microglia integrative analysis where each cell is colored by its dataset of origin.* ***C)*** *Proportion of microglial states stratified by brain region.* ***D)*** *Marker expression consistency of previous human and mouse single-cell datasets with the biopsy dataset. Consistency score is defined as the fraction of markers from human*

biopsy dataset for each microglia state that show a conserved up- or down-regulation pattern in each dataset. ***E)*** *The fraction of DE genes from the biopsy dataset between each pair of microglia states that have a conserved logFC pattern (e.g., up or down in both cell states). DE genes were calculated by comparing Aβ+/Aβ+Tau+ samples with controls.* ***F)*** *Comparison of DE genes between GPNMB-LPL and CX3CR1 microglia types in the biopsy dataset. The analysis is based on the union of top 300 DE genes in each cell type to reduce the impact of cell type size variation (i.e., statistical power).* ***G)*** *Microglia DE genes from the biopsy dataset are upregulated in two AD postmortem studies and are enriched for the markers of GPNMB-LPL and LPL-CD83 microglia states. Meta-gene expression of the up-regulated microglial DE genes from our dataset in two published postmortem studies[4,6]. The meta-gene was constructed by summing their UMI counts in each cell and normalizing by the nUMI. The gray lines illustrate the median expression of the meta-gene across microglia states.* ***H)*** *Differential expression analysis of astrocyte genes in response to Microglia GPNMB-EYA2 and LPL-CD83 expansion. The DE genes (FDR-adjusted p-value < 0.05) are represented in red. Fractions of microglia GPNMB-EYA2 and LPL-CD83 cells in individuals are normalized using an empirical normal cumulative estimation function (ecdf function in R) to have a range between zero and one.* ***I)*** *Enrichment of mouse microglia states in response to various conditions (Fisher's exact test; FDR-adjusted p-value < 0.1).*

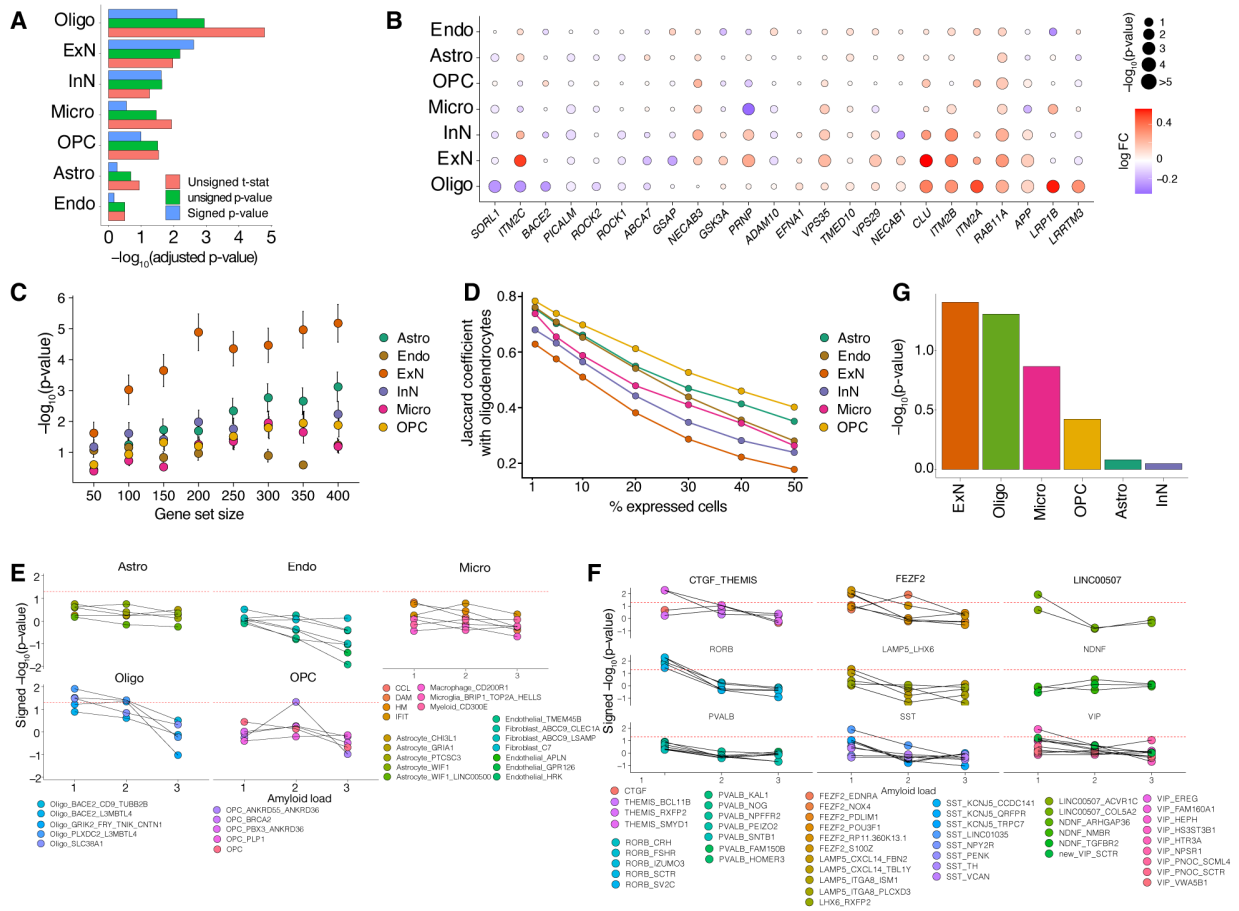

Figure S9. Nomination of amyloid-producing cell types in the human frontal cortex

A) *Bar chart showing -log$_{10}$-transformed p-values for various ordering statistics (indicated at bottom right) based on GSEA of Aβ production and secretion geneset (**Table S7**) and cell class DE genes.* ***B)*** *Dot plot denoting differential expression of leading edge genes, identified by the GSEA of Aβ gene set in **Figure 5A**, in Aβ+ subjects versus Aβ-free biopsy samples. Color correlates with log-fold change and size correlates to -log$_{10}$-transformed p-values.* ***C)*** *Correlation analysis results obtained via fGSEA (see **Methods**) comparing differentially expressed gene lists between all major cell classes and oligodendrocytes, with increasingly liberal thresholds (larger gene lists) for assigning univariate significance.* ***D)*** *Overlap of genes expressed in oligodendrocytes with other major cell classes. Different thresholds were selected to consider a gene as expressed (x-axis) based on the percentage of the cells in which the gene has non-zero UMI.* ***E,F)*** *Signed -log$_{10}$-transformed p-values associated with fGSEA enrichment across increasing Aβ and tau burdens for all major cell types (glia in **(E)** and neurons in **(F)**) in human frontal cortex from DE analysis of the human biopsy dataset.* ***G)*** *Meta-analysis p-values for fGSEA of the Aβ associated gene set in the DE genes of two postmortem AD case-control datasets [3,4], for six cell classes.*

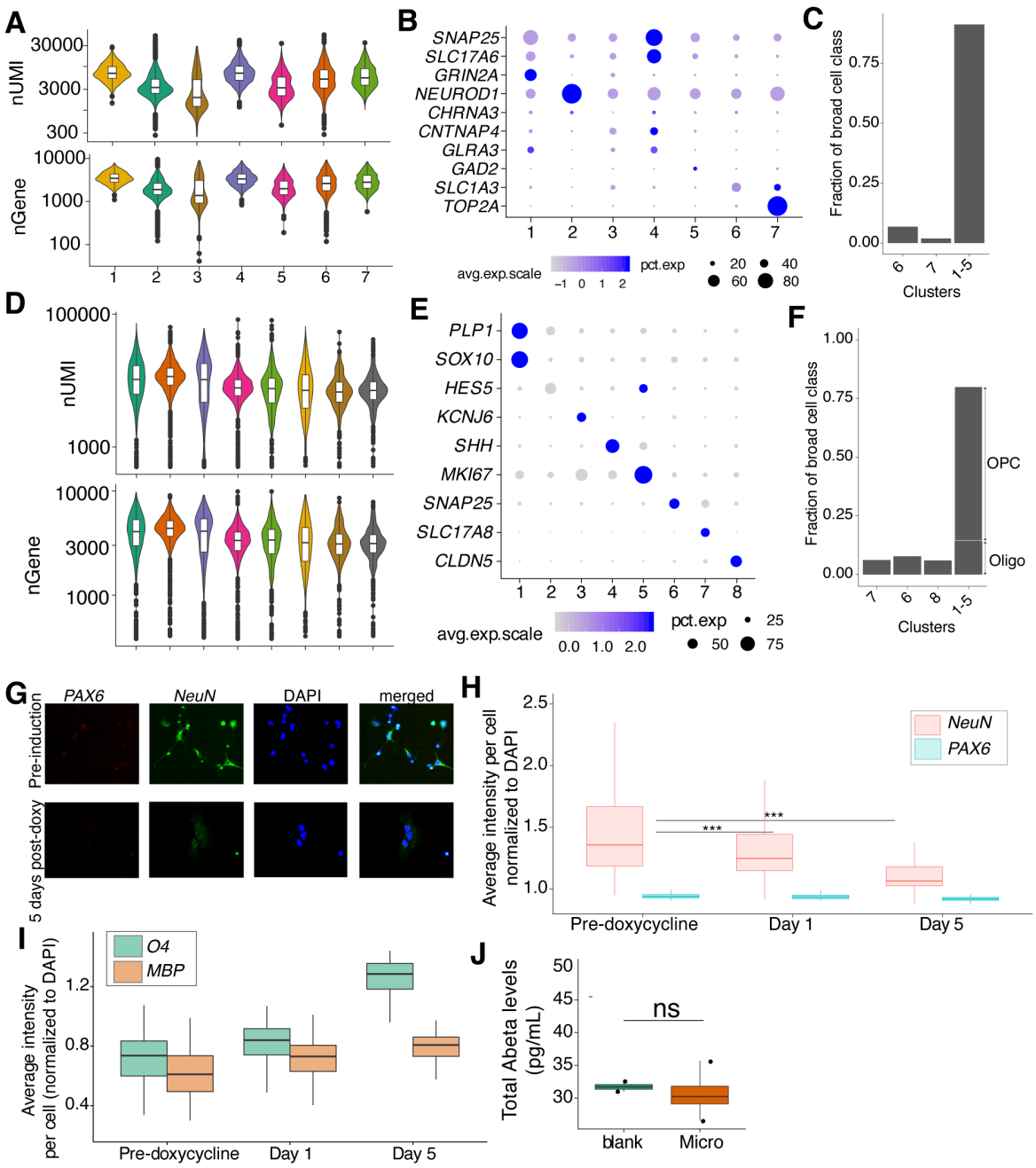

Figure S10. Single-cell transcriptomics and immunohistochemistry of ESC-derived oligodendrocyte and neuron cultures

A,D) *Violin plot of number of nUMI (top) and nGene (bottom) per cell type identified in single-cell transcriptomics of ESC-derived iExN (**A**) and (**D**) iOligo lineage cultures. In boxplots, center line, median; box limits, upper and lower quartiles; whiskers, 1.5x interquartile range; points, outliers.* ***B,E)*** *Key marker genes for cell types identified from single-cell transcriptomics of ESC-derived iExN (**B**) and (**E**) iOligo cultures.* ***C,F)*** *Composition of ESC-derived iExN (**C**) and iOligo (**F**) cultures based upon single-cell cluster annotations.* ***G)*** *Representative images of immunofluorescence stains of PAX6 and NeuN (**G**) in ESC-derived iOligo cultures.* ***H,I)*** *Box plots of average intensity values per cell (normalized to DAPI intensity) across days of differentiation for NeuN, PAX6 (**H**), O4, and MBP (**I**). Box upper and lower bounds represent upper and lower quartiles and Whisker distance from upper and lower hinges represents ≤1.5*

times the interquartile range. Center line indicates the median value. ***J)*** *Total Aβ levels from conditioned media isolated from ESC-derived microglia and blank control derived from unconditioned oligodendrocyte differentiation media. *** = p < 0.001, ** = p < 0.01, * = p < 0.05, NS = not significant. Statistical tests are based on a linear mixed-effect model for comparing immunofluorescence signal intensity per cell using each sample well as the levels of the random effect. Statistical significance for comparing amyloid beta protein values was determined via the Student's t-test.*